IEEE Access
Multidisciplinary | Rapid Review | Open Access Journal

Received 14 April 2023, accepted 8 June 2023, date of publication 19 June 2023, date of current version 26 June 2023.

Digital Object Identifier 10.1109/ACCESS.2023.3287224

RESEARCH ARTICLE

A Data-Assimilation Based Method for Equilibrium Reconstruction of Magnetic Fusion Plasma: Solution by Adjoint Method

AKIO SANPEI[1], (Member, IEEE), SADAO MASAMUNE[1,2], AND YASUAKI KUROE[1,3], (Life Member, IEEE)

[1]Department of Electronics, Kyoto Institute of Technology, Kyoto 606-8585, Japan
[2]College of Engineering, Chubu University, Kasugai 487-8501, Japan
[3]Mobility Research Center, Doshisha University, Kyoto 602-8580, Japan

Corresponding author: Akio Sanpei (sanpei@kit.ac.jp)

This work was supported in part by the Kansai Research Foundation for Technology Promotion, in 2018; in part by the National Institute for Fusion Science under Grant NIFS20KOAP035 and Grant NIFS22KIPP015; and in part by the Japan Society for the Promotion of Science KAKENHI under Grant 22K04172, Grant 20KK0063, and Grant 21H01056.

ABSTRACT Accurately determining the magnetohydrodynamic (MHD) equilibrium is fundamentally important in controlling and stabilizing fusion plasmas. Development of reliable methods for equilibrium reconstruction is therefore crucial to advancing the fusion plasma research. However, since the dynamics of plasma phenomena are highly nonlinear and highly complicated dynamics, it is difficult to develop their rigorous mathematical model. We already proposed a method of equilibrium reconstruction for fusion plasmas based on data assimilation. In the method the problem is formulated as a parameter optimization and a solution by the sensitivity equation method is proposed. In this paper, we propose a solution of equilibrium reconstruction for fusion plasmas by the adjoint method for the purpose of reducing computation time. In order to ensure the applicability of the adjoint method to a wide class of fusion plasmas, the problem formulation and derivation of the reconstruction algorithm based on the adjoint method are performed in generic form. Furthermore, we implement the proposed method as equilibrium reconstruction algorithms applicable to axisymmetric toroidal plasmas, typical examples of which are tokamaks and reversed field pinches (RFPs). Finally, the proposed method is applied to a real RFP experiment, and it is shown that the proposed method has the capability of reconstructing the equilibrium with sufficient accuracy and dramatic reduction of computation time compared with the existing methods.

INDEX TERMS Fusion plasma, equilibrium reconstruction, data assimilation, adjoint method.

I. INTRODUCTION

In view of the recent rapid progress of global warming, it has become an urgent need to develop suitable energy sources with zero carbon dioxide emission. Nuclear fusion energy is one of the candidates for such energy sources [1], [2], and development of nuclear fusion reactor has been in progress to realize electric energy production. ITER (''The Way'' in Latin) tokamak is under construction as an international collaboration program, whose initial fusion experiment is scheduled to start in 2035 [3]. Under these circumstances, developments of reliable methods of plasma modeling, analysis, design, and simulation are becoming urgent issues to predict the performance of the produced fusion plasmas, to establish control methods, and to develop operation scenarios. However, plasma phenomena include a wide variety of physical phenomena over a very wide range of time and space scales, and they have complicated nonlinearities. Therefore, rigorous theoretical treatment of plasma phenomena is extremely difficult. Because of these difficulties, many problems remain to be solved and one of them is the problem of reconstructing the equilibrium state of the plasma. This

The associate editor coordinating the review of this manuscript and approving it for publication was Roberta Palmeri.

problem is an inverse problem of determining the equilibrium state of plasma under given conditions, and is fundamental to the development of control methods to maintain plasma stability. In this paper we deal with the equilibrium reconstruction problem of magnetic fusion plasmas.

In magnetic fusion plasmas, when there exist magnetic surfaces, the equilibrium state is modeled by some partial differential equations with respect to some magnetic quantities such as flux functions, and the equilibrium state can be obtained by solving them given boundary conditions [4], [5], [6]. However, the actual magnetic fusion plasma contains so many unknown elements and the boundary conditions are so complex that it is almost impossible to develop its rigid mathematical model, which makes it extremely difficult to obtain the equilibrium state with necessary accuracy. In such cases, measurement data obtained from sensors equipped with the plasma device are used to solve the partial differential equation representing the equilibrium state in order to reconstruct the equilibrium state of the plasma.

Meanwhile, for simulation and estimation problems of large and complex systems, it is often not possible to obtain a rigid mathematical model of target systems, and in such cases, research on data assimilation, which supplements the simulation with data obtained from equipped devices such as sensors, is being studied. In the last decades, data assimilation has attracted much attention especially in simulating and estimating large-scale complex systems. There have been several methods and algorithms developed, and a lot of efforts have been made for applying them to solving inverse problems in various fields from environmental sciences, atmospheric sciences, geosciences, and biology to human and social sciences [7], [8], [9], [10], [11]. The purpose of this paper is to develop a method for reconstructing the equilibrium state of magnetic fusion plasmas based on data assimilation.

In axisymmetric toroidal plasmas, typical examples of which are the tokamak and reversed field pinch (RFP) plasmas, the equilibrium is modeled by a partial differential equation with respect to the poloidal flux function [4], [5]. In equilibrium reconstruction methods for tokamak plasmas, the unknown parts can be parametrized by some linear functions with respect to unknown parameters, which makes it easier to seek for values of those parameters that best reproduce the experimental observations. This type of parametrization has been widely used in equilibrium reconstruction for tokamak plasmas with so many publications [12], [13], [14], [15], [16], [17], [18], [19], [20]. Further improvements of the existing reconstruction methods are in progress, for example, by investigating appropriateness of the parametrization [21], and/or by elaboration on modeling the complicated boundary conditions [22]. On the other hand, in the present equilibrium reconstruction methods for RFP plasmas, parametrization of the unknown parts is somewhat different from that for tokamaks [23], [24] mainly because of the different nature of the equilibrium; the RFP equilibrium is sustained by small-scale fluctuations around a time-averaged equilibrium state [25], [26]. It is therefore important for RFP equilibrium reconstruction to develop appropriate parametrization of the unknown parts.

As mentioned earlier, the studies on data assimilation are being conducted in a variety of fields and it is necessary to develop new methods on data assimilation for the specific problems of each field. For the problem of equilibrium reconstruction of fusion plasma, we have presented its problem formulation as data assimilation and proposed a new method to solve the problem [23]. In the proposed method the reconstruction problem is formulated as an optimization problem and the sensitivity equation is derived to solve it. In this paper, we propose a method for equilibrium reconstruction based on data assimilation by deriving the adjoint equation and developing an algorithm, in order to reduce computation time much more than that of our previous work [23]. The adjoint method has attracted much attention in data assimilation since the inverse problem is usually formulated as an optimization problem. Features of the proposed method are as follows. (i) In order to emphasize the applicability of the proposed method to a wide class of magnetic fusion plasmas including tokamak and RFP, the mathematical formulation is performed in generic form, not specifying the model partial differential operator in the model equation. In particular, the effect of the magnetic axis is taken into account in mathematical formulation both in the original model equation and the adjoint equation. (ii) An adjoint operator is derived for axisymmetric configuration, and an algorithm for equilibrium reconstruction is developed for axisymmetric toroidal plasmas. Since the model partial differential equation for axisymmetric plasmas is common to the tokamak and RFP, the developed algorithm is also applicable to both of these plasmas.

The proposed method for reconstruction is applied to a real RFP plasma in order to evaluate the proposed method by quantitatively comparing the reconstruction results with those in our previous publication [23], and conducted two experiments. In the first experiment, in order to evaluate the accuracy of the proposed method, the numerical experiment is performed in which the algorithm is applied to simulated numerical data. It is confirmed that the proposed method provides the reconstructed results with the same accuracy as that in our previous method, with much small amount of computation time. In the second experiment the algorithm is applied to the real experimental data obtained in an RFP experimental device (REversed field Pinch of Low-Aspect-ratio eXperiment (RELAX)) [27] developed at Kyoto Institute of Technology. It is shown that the proposed method makes it possible to reconstruct the equilibrium state of plasma appropriately and quite efficiently.

The rest of the paper is organized as follows. In section II, the problem of equilibrium reconstruction is formulated in generic form. In section III, a reconstruction algorithm by adjoint method is proposed. In section IV, the proposed

reconstruction method is applied to axisymmetric toroidal plasmas by deriving the adjoint equation. In section V, the proposed algorithm is applied to a real RFP experiment. Conclusion of the present work is given in section VI.

II. PROBLEM FORMULATION of EQUILIBRIUM RECONSTRUCTION AS DATA ASSIMILATION

In this section, we formulate the equilibrium reconstruction problem as data assimilation for magnetic fusion plasma. In the previous paper, we considered a system described by the following partial differential equation and associated boundary condition in the three-dimensional space $\boldsymbol{R}^3$ [23].

$$\mathcal{L}_k \psi_k(\boldsymbol{x}) = f_k^o(\boldsymbol{x}, \psi_1(\boldsymbol{x}), \psi_2(\boldsymbol{x}), \cdots, \psi_K(\boldsymbol{x})), \quad \boldsymbol{x} \in \boldsymbol{D} \subset \boldsymbol{R}^3, \quad k = 1, 2, \cdots, K \tag{1}$$

where $\psi_k \in \boldsymbol{R}$ is the scalar quantity characterizing the equilibrium state of the fusion plasma, $\mathcal{L}_k$ is a partial differential operator with respect to the spatial variable $\boldsymbol{x}$ including high order partial derivatives. $\boldsymbol{D}$ $\left(\subset \boldsymbol{R}^3\right)$ is an open region in which the scalar function $\psi_k(\boldsymbol{x})$ is defined. f_k^o is a nonlinear function $(f_k^o : \boldsymbol{R}^3 \times \underbrace{\boldsymbol{R} \times \cdots \times \boldsymbol{R}}_{K} \to \boldsymbol{R})$. For an axisymmetric toroidal plasma such as standard tokamak or RFP, the equilibrium is described by a single partial differential equation ($K = 1$). For a non-axisymmetric plasma, if the magnetic surfaces exist, the plasma equilibrium can be described by a set of nonlinear partial differential equations with respect to three scalar functions ($K = 3$) [6].

In this paper we set $K = 1$ for simplicity. We start with the following equation to describe the equilibrium

$$\mathcal{L}\psi(\boldsymbol{x}) = f^o(\boldsymbol{x}, \psi(\boldsymbol{x})), \quad \boldsymbol{x} \in \boldsymbol{D} \subset \boldsymbol{R}^3. \tag{2}$$

The proposed method, which will be explained in the following sections, can be extended to the system described by (1) where $K > 1$ straightforwardly.

The boundary condition of the partial differential equation (2) is given as follows.

$$f^{Bo}(\psi(\boldsymbol{x})) = 0, \quad \boldsymbol{x} \in \partial \boldsymbol{D}, \tag{3}$$

where $\partial \boldsymbol{D}$ is the boundary of the region $\boldsymbol{D}$ and f^{Bo} is a nonlinear function $\left(f^{Bo} : \boldsymbol{R} \to \boldsymbol{R}\right)$. Since the operator $\mathcal{L}$ includes high order derivatives with respect to spatial variable $\boldsymbol{x}$, the boundary condition could include the derivatives of ψ. For simplicity, we consider that f^{Bo} is a function of only $\psi(\boldsymbol{x})$. It should be noted that it is easy to extend our discussions in the case that the system (2) has such general boundary conditions.

The equilibrium reconstruction problem is to obtain the solution of the partial differential equation (2) with the boundary condition (3) for given functions f^o and f^{Bo}. However it is almost impossible to give these functions exactly in actual magnetic fusion plasma. We introduce the concept of data assimilation to the equilibrium reconstruction problem. By using the information obtained from several sensors attached to the plasma device, the problem is formulated as follows. Introducing an adjustable vector parameter, we parameterize uncertainties and unknowns in f^o and f^{Bo}. Let $\boldsymbol{p} = [p_1, \cdots, p_{N_p}]^t$ be the adjustable parameter vector whose number of elements is N_p. We call $p_i (i = 1, \cdots, N_p)$ the free parameters. By the parametrization, (2) and (3) become:

$$\mathcal{L}\psi(\boldsymbol{x}, \boldsymbol{p}) = f(\boldsymbol{x}, \psi(\boldsymbol{x}, \boldsymbol{p}), \psi(\boldsymbol{x}_{ex}), \boldsymbol{p}) \quad \boldsymbol{x} \in \boldsymbol{D} \subset \boldsymbol{R}^3. \tag{4}$$

where $\boldsymbol{x}_{ex} \in \boldsymbol{D}$ is a point where the gradient of ψ takes a known value $\boldsymbol{c}$ as follows,

$$\frac{\partial \psi}{\partial \boldsymbol{x}}(\boldsymbol{x}_{ex}) = \boldsymbol{c}, \tag{5}$$

and

$$f^B(\psi(\boldsymbol{x}), \boldsymbol{p}) = 0, \quad \boldsymbol{x} \in \partial \boldsymbol{D}. \tag{6}$$

The condition (5) appears by parametrization of the target equation. For example, $\boldsymbol{x}_{ex}$ is a point where $\psi(\boldsymbol{x})$ takes an extremum in the region $\boldsymbol{D}$ if $\boldsymbol{c} = \boldsymbol{0}$. In parameterizations, in general, the scalar quantity $\psi(\boldsymbol{x})$ is often normalized by its maximum or minimum value, which brings the condition (5). The equilibrium reconstruction problem based on data assimilation in this paper is to solve the partial differential equations (4) and (5) under the boundary condition (6) and to obtain the free parameter $\boldsymbol{p}$ simultaneously.

The free parameter $\boldsymbol{p}$ will be determined by using the data obtained from sensors as follows. Let N_m be the number of sensors attached to the plasma device and d_i, the data from the i-th sensor ($i = 1, 2, \cdots, N_m$). Suppose that the sensing process of the i-th sensor is modeled mathematically by the following equation

$$m_i = \mathscr{F}_{m_i}(\psi(\boldsymbol{x}), \boldsymbol{p}) \quad i = 1, 2, \cdots, N_m \tag{7}$$

where $\mathscr{F}_{m_i}$ is an operator mapping from $L(\boldsymbol{D}) \times N_p$ to $\boldsymbol{R}$, and $L(\boldsymbol{D})$ is an appropriate function space defined in the region $\boldsymbol{D}$, and m_i is the output of the i-th sensing process. For example, $\mathscr{F}_{m_i}$ is a weighted integral operator over the sensing area. If the weighting function is the delta function, $\mathscr{F}_{m_i}$ corresponds to one point measurement process. We will determine the free parameter $\boldsymbol{p}$ such that the outputs m_i of the sensing process (7) best reproduce the real data d_i. Define the following cost function

$$E(\boldsymbol{p}) = \frac{1}{2}\sum_{i=1}^{N_m} w_i e_i^2 = \frac{1}{2}\sum_{i=1}^{N_m} w_i (m_i - d_i)^2 \tag{8}$$

where $w_i \geq 0$ is a weighting coefficient. The problem of data assimilation is reduced to finding the parameter $\boldsymbol{p}$ which minimizes the cost function (8) under the constraints (4), (5), (6) and (7). It is formulated as the following optimization problem with equality constraints.

$$\begin{aligned} &\underset{\boldsymbol{p}}{\text{minimize}}\ E(\boldsymbol{p}) \\ &\text{subject to (4), (5), (6) and (7).} \end{aligned} \tag{9}$$

The solution of (4), (5) and (6) for the optimal parameter of the above optimization problem is the equilibrium state of the target plasma which best reproduces experimental data.

III. PROPOSED RECONSTRUCTION METHOD BY ADJOINT METHOD

The constrained optimization problem (9) can be solved by using a gradient-based method such as the steepest descent method, conjugate gradient method, quasi-Newton method, and so on. In these algorithms, the gradient of the cost function (8) with respect to $\boldsymbol{p}$, denoted by $\partial E/\partial \boldsymbol{p}$, has to be calculated. For this purpose we have already proposed a method of derivation of the gradients based on the sensitivity equations [23]. In this paper we propose a computationally more efficient method based on the adjoint equation. We start with revisiting derivation of the sensitivity equations in [23], and then, derive the adjoint equation on the basis of the sensitivity equations.

A. REVISITNG DERIVATION of SENSITIVITY EQUATION

The gradient of the cost function $E(\boldsymbol{p})$ for the free parameter $\boldsymbol{p}$ is obtained by differentiating (8) for p_j, the j-th element of $\boldsymbol{p}$, as follows,

$$\frac{\partial E}{\partial p_j} = \sum_{i=1}^{N_m} w_i e_i \frac{\partial e_i}{\partial p_j} = \sum_{i=1}^{N_m} w_i e_i \frac{\partial m_i}{\partial p_j}. \tag{10}$$

The terms $\partial m_i/\partial p_j$ in (10) are obtained by differentiating (7) for p_j,

$$\frac{\partial m_i}{\partial p_j} = \frac{\partial \mathscr{F}_{m_i}}{\partial \psi}\frac{\partial \psi}{\partial p_j} + \frac{\partial \mathscr{F}_{m_i}}{\partial p_j}, \quad i = 1, 2, \cdots, N_m. \tag{11}$$

The terms $\partial \psi/\partial p_j$ appearing in (11) are called the sensitivity, which are the solutions to the following sensitivity equations, and essentially the equations are obtained by differentiating (4) for p_j,

$$\begin{aligned}\mathcal{L}\frac{\partial \psi}{\partial p_j} = \frac{\partial f}{\partial \psi}\frac{\partial \psi}{\partial p_j} + \frac{\partial f}{\partial \psi(\boldsymbol{x}_{ex})}\Bigg(\frac{\partial \psi(\boldsymbol{x}_{ex})}{\partial p_j} \\ - \frac{\partial \psi(\boldsymbol{x}_{ex})}{\partial \boldsymbol{x}}\frac{\partial^2 \psi(\boldsymbol{x}_{ex})}{\partial \boldsymbol{x}^2}^{-1}\frac{\partial}{\partial \boldsymbol{x}}\frac{\partial \psi(\boldsymbol{x}_{ex})}{\partial p_j}\Bigg) + \frac{\partial f}{\partial p_j}, \\ \boldsymbol{x} \in \boldsymbol{D} \subset \boldsymbol{R}^3.\end{aligned} \tag{12}$$

For the details of derivation of the sensitivity equations, refer to [23].

As is clear from (10), in obtaining the gradient of the cost function, $\partial E/\partial p_j$, we solve the sensitivity equations (12) in order to obtain $\partial \psi/\partial p_j$, the total number of which is N_p, being equal to the number of the free parameters p_j. Then we put the solutions $\partial \psi/\partial p_j$ into (10). In contrast, in the adjoint method proposed in this paper, as will be explained below, the gradient of the cost function $\partial E/\partial \boldsymbol{p}$ is calculated from a single variable, called adjoint variable, which is obtained by solving a single partial differential equation, named as adjoint equation.

B. DERIVATION OF ADJOINT EQUATION AND PROCEDURE OF THE PROPOSED METHOD

Consider the appropriate function space defined on $\boldsymbol{D} \subset \boldsymbol{R}^3$ whose member functions are applicable of the partial differential operator $\mathcal{L}$ and satisfy the boundary condition (3). We define the inner product of its member functions $\psi(\boldsymbol{x})$ and $\chi(\boldsymbol{x})$ as follows:

$$< \psi(\boldsymbol{x}), \chi(\boldsymbol{x}) >= \int_D \psi(\boldsymbol{x})\chi(\boldsymbol{x})d\boldsymbol{x} \tag{13}$$

We suppose here that the sensing processes (7) are expressed by the following equation.

$$m_i = \mathscr{F}_{m_i}(\psi(\boldsymbol{x}), \boldsymbol{p}) = \int_D f_{m_i}(\psi(\boldsymbol{x}), \boldsymbol{p})d\boldsymbol{x}, \quad i = 1, 2, \cdots, N_m. \tag{14}$$

Then, using the inner product, $\partial m_i/\partial p_j$ and $\partial E/\partial p_j$ can be expressed as follows.

$$\begin{aligned}\frac{\partial m_i}{\partial p_j} &= \int_D \Big(\frac{\partial f_{m_i}}{\partial \psi}\frac{\partial \psi}{\partial p_j} + \frac{\partial f_{m_i}}{\partial p_j}\Big)d\boldsymbol{x} \\ &=< \frac{\partial f_{m_i}}{\partial \psi}, \frac{\partial \psi}{\partial p_j} > + \int_D \frac{\partial f_{m_i}}{\partial p_j}d\boldsymbol{x} \\ &\quad i = 1, 2, \cdots, N_m\end{aligned} \tag{15}$$

$$\frac{\partial E}{\partial p_j} = \sum_{i=1}^{N_m} w_i e_i \left(< \frac{\partial f_{m_i}}{\partial \psi}, \frac{\partial \psi}{\partial p_j} > + \int_D \frac{\partial f_{m_i}}{\partial p_j}d\boldsymbol{x}\right). \tag{16}$$

In order to derive the adjoint equation and adjoint variable, taking the inner product of a certain member function $\hat{\psi}(\boldsymbol{x})$ and both sides of (12), we obtain the following equation,

$$\begin{aligned}< \mathcal{L}\frac{\partial \psi}{\partial p_j}, \hat{\psi}(\boldsymbol{x}) > =< \frac{\partial f}{\partial \psi}\frac{\partial \psi}{\partial p_j} + \frac{\partial f}{\partial \psi(\boldsymbol{x}_{ex})}\partial f_{ex}\delta(\boldsymbol{x} - \boldsymbol{x}_{ex}) \\ \times \frac{\partial \psi}{\partial p_j}, \hat{\psi}(\boldsymbol{x}) > + < \frac{\partial f}{\partial p_j}, \hat{\psi}(\boldsymbol{x}) >\end{aligned} \tag{17}$$

where the operator ∂f_{ex}, defined by the following relation, is introduced for the sake of simplicity,

$$\partial f_{ex} = 1 - \frac{\partial \psi(\boldsymbol{x}_{ex})}{\partial \boldsymbol{x}}\frac{\partial^2 \psi(\boldsymbol{x}_{ex})}{\partial \boldsymbol{x}^2}^{-1}\frac{\partial}{\partial \boldsymbol{x}}. \tag{18}$$

Using the adjoint operator $\hat{\mathcal{L}}$, which satisfies the following relation for the two member functions $\psi(\boldsymbol{x})$ and $\hat{\psi}(\boldsymbol{x})$,

$$< \mathcal{L}\psi(\boldsymbol{x}), \hat{\psi}(\boldsymbol{x}) >=< \psi(\boldsymbol{x}), \hat{\mathcal{L}}\hat{\psi}(\boldsymbol{x}) > \tag{19}$$

the left-hand side of (17) can be replaced by the right-hand side of the following relation,

$$< \mathcal{L}\frac{\partial \psi}{\partial p_j}, \hat{\psi}(\boldsymbol{x}) >=< \frac{\partial \psi}{\partial p_j}, \hat{\mathcal{L}}\hat{\psi}(\boldsymbol{x}) > . \tag{20}$$

Using this relation (17) can be rewritten as follows,

$$< \frac{\partial \psi}{\partial p_j}, \hat{\mathcal{L}}\hat{\psi}(\boldsymbol{x}) - \frac{\partial f}{\partial \psi}\hat{\psi}(\boldsymbol{x}) - \frac{\partial f}{\partial \psi(\boldsymbol{x}_{ex})}\partial\hat{f}_{ex}\delta(\boldsymbol{x}-\boldsymbol{x}_{ex})\hat{\psi}(\boldsymbol{x}) > =< \frac{\partial f}{\partial p_j}, \hat{\psi}(\boldsymbol{x}) > \tag{21}$$

where $\partial\hat{f}_{ex}$ is the adjoint operator to ∂f_{ex} satisfying the following relation,

$$< \partial f_{ex}\delta(\boldsymbol{x}-\boldsymbol{x}_{ex})\psi(\boldsymbol{x}), \hat{\psi}(\boldsymbol{x}) > =< \psi(\boldsymbol{x}), \partial\hat{f}_{ex}\delta(\boldsymbol{x}-\boldsymbol{x}_{ex})\hat{\psi}(\boldsymbol{x}) > . \tag{22}$$

Adding the left- and right-hand sides of (16) to the left- and right-hand sides of (21) respectively, and rearranging some terms, we obtain

$$\frac{\partial E}{\partial p_j} + < \frac{\partial \psi}{\partial p_j}, \hat{\mathcal{L}}\hat{\psi}(\boldsymbol{x}) - \frac{\partial f}{\partial \psi}\hat{\psi}(\boldsymbol{x}) - \frac{\partial f}{\partial \psi(\boldsymbol{x}_{ex})}\partial\hat{f}_{ex}\delta(\boldsymbol{x}-\boldsymbol{x}_{ex})\hat{\psi}(\boldsymbol{x}) - \sum_{i=1}^{N_m} w_i e_i \frac{\partial f_{m_i}}{\partial \psi} > =< \frac{\partial f}{\partial p_j}, \hat{\psi}(\boldsymbol{x}) > + \sum_{i=1}^{N_m} w_i e_i \int_D \frac{\partial f_{m_i}}{\partial p_j} d\boldsymbol{x}. \tag{23}$$

When the certain member function $\hat{\psi}(\boldsymbol{x})$ in (23) is a solution to the following partial differential equation and satisfies the boundary condition (3),

$$\hat{\mathcal{L}}\hat{\psi}(\boldsymbol{x}) = \frac{\partial f}{\partial \psi}\hat{\psi}(\boldsymbol{x}) + \frac{\partial f}{\partial \psi(\boldsymbol{x}_{ex})}\partial\hat{f}_{ex}\delta(\boldsymbol{x}-\boldsymbol{x}_{ex})\hat{\psi}(\boldsymbol{x}_{ex}) + \sum_{i=1}^{N_m} w_i e_i \frac{\partial f_{m_i}}{\partial \psi} \tag{24}$$

$$f^{Bo}(\hat{\psi}(\boldsymbol{x})) = 0 \quad \boldsymbol{x} \in \partial \boldsymbol{D} \tag{25}$$

then, the bracket term (the second term) in the left-hand side of (23) diminishes, and the gradient of the cost function $\partial E/\partial p_j$ can be represented by the single variable $\hat{\psi}(\boldsymbol{x})$ as follows,

$$\frac{\partial E}{\partial p_j} =< \frac{\partial f}{\partial p_j}, \hat{\psi}(\boldsymbol{x}) > + \sum_{i=1}^{N_m} w_i e_i \int_D \frac{\partial f_{m_i}}{\partial p_j} d\boldsymbol{x}. \tag{26}$$

The partial differential equation (24) is called the adjoint equation and the solution $\hat{\psi}(\boldsymbol{x})$ to the adjoint equation satisfying the boundary condition (25) is called the adjoint variable.

The optimization problem (9) can be solved by using the $\partial E/\partial p_j$ thus obtained. The procedure of equilibrium reconstruction in the proposed method is summarized in Fig. 1.

Note that $\boldsymbol{c} = 0$ in (5) in the mathematical model of the target RFP plasma as shown in the next section. In this case,

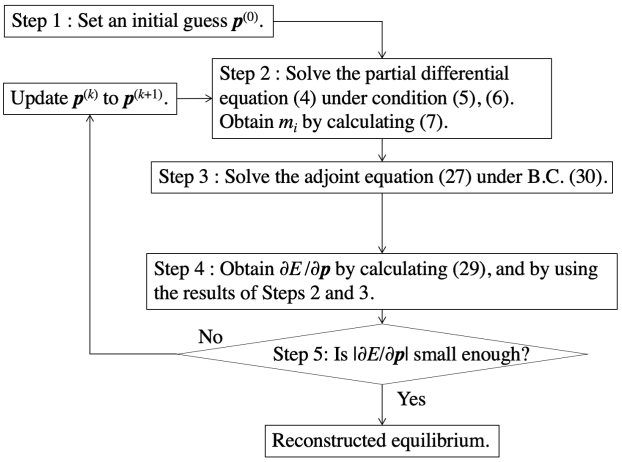

FIGURE 1. Flowchart of the procedure of the proposed method.

∂f_{ex} defined by (18) becomes 1, and the adjoint equation (24) becomes

$$\hat{\mathcal{L}}\hat{\psi}(\boldsymbol{x}) = \frac{\partial f}{\partial \psi}\hat{\psi}(\boldsymbol{x}) + \frac{\partial f}{\partial \psi(\boldsymbol{x}_{ex})}\delta(\boldsymbol{x}-\boldsymbol{x}_{ex})\hat{\psi}(\boldsymbol{x}_{ex}) + \sum_{i=1}^{N_m} w_i e_i \frac{\partial f_{m_i}}{\partial \psi}. \tag{27}$$

Remark 1: The calculation method of the gradient $\partial E/\partial p_j$ used in [23] requires solving partial differential equations, the sensitivity equations, the total number of which is N_p. On the other hand, the method proposed in this paper requires solving only single partial differential equation, the adjoint equation, to obtain the gradient. Therefore, the proposed method based on the adjoint equation is expected to reduce the computational time drastically compared to the method based on the sensitivity equation in [23]. The advantage of the proposed method will become more pronounced as the number of free parameters increases.

IV. PROPOSED RECONSTRUCTION METHOD FOR AXISYMMETRIC TOROIDAL PLASMA

There are two magnetic confinement configurations in axisymmetric toroidal plasmas; one is the tokamak, and the other is the RFP. The equilibrium is described by the Grad-Shafranov (GS) equation [4], [5]. In this section, we deal with the equilibrium state of axisymmetric magnetic fusion plasma as a target. We propose a method for implementation of the equilibrium reconstruction algorithm with the adjoint equation described in the previous section.

The rest of this section is organized as follows. In Sec. IV-A, the mathematical model of axisymmetric toroidal plasma will be described. In Sec. IV-B, we will derive the adjoint equation for the plasma. In Sec. IV-C, a method for implementation of the equilibrium reconstruction algorithm will be proposed.

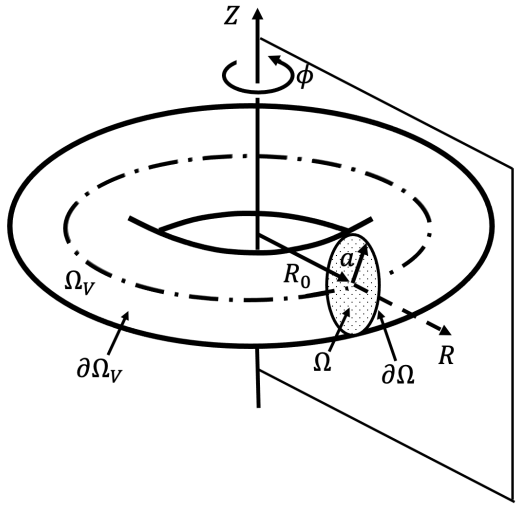

FIGURE 2. Toroidal plasma and the cylindrical coordinate system.

A. MATHEMATICAL MODEL OF EQUILIBRIUM of AXISYMMETRIC TOROIDAL PLASMA

The axisymmetric system has rotational symmetry around an axis, which is denoted by Z, and the cylindrical coordinate system with Z axis is usually used to describe the axisymmetric plasma. Figure 2 shows the schematic drawing of a toroidal plasma and its cylindrical coordinate system (R, ϕ, Z). Let R_0 (major radius) be the distance from the Z axis to the geometric center of the torus small circle, and the radius of the small circle be a (minor radius). Ω_V and $\partial\Omega_V$ are the 3D plasma domain and its surface, respectively. Ω and $\partial\Omega$ are their projection on a poloidal plane, that is, the 2D plasma domain and its boundary, respectively. The plasma is confined by a toroidal magnetic field B_ϕ in the toroidal direction and a poloidal magnetic field B_p in the (R, Z) plane which will be referred to as the poloidal plane. B_ϕ is partly applied externally and partly produced by the internal poloidal plasma current, while B_p is formed by the toroidal plasma current I_ϕ, whose current density is denoted by J_ϕ. The plasma equilibrium is a state where the pressure gradient force balances the electromagnetic force, that is, the equilibrium is described by the plasma pressure and the magnetic field. For plasma with axisymmetry, the pressure and the poloidal magnetic field are shown to be a function of the poloidal magnetic flux function ψ which is a function of R and Z.

Therefore, the model (2) descibing the equilibrium for axisymmetric toroidal plasmas is represented as follows [4], [5].

$$\begin{aligned} \Delta^*\psi(R,Z) &= -\mu_0 R J_\phi(\psi(R,Z),R,Z), \\ J_\phi(\psi(R,Z),R,Z) &= \frac{F(\psi(R,Z))F'(\psi(R,Z))}{\mu_0 R} \\ &\quad + RP'(\psi(R,Z)), \quad (R,\phi,Z)\in\Omega_V \end{aligned} \tag{28}$$

where F is the poloidal current function $F(\psi(R,Z)) = RB_\phi(R,Z)$ and $P(\psi(R,Z))$ is the pressure function. In the above equation, $F'$and P' are $F' = dF/d\psi$ and $P' = dP/d\psi$. The differential operator Δ^* is given by

$$\Delta^* = \frac{\partial^2}{\partial R^2} - \frac{1}{R}\frac{\partial}{\partial R} + \frac{\partial^2}{\partial Z^2}. \tag{29}$$

The boundary condition for (28) is a fixed boundary given as

$$\psi(R,Z) = c\ (constant) \quad (R,Z)\in\partial\Omega \tag{30}$$

The constant c in (30) is chosen to be 0, which means that the poloidal flux is defined by taking the boundary $\partial\Omega$ as a reference. The partial differential equation (28) is the GS equation.

B. DEVIATION of ADJOINT EQUATION

Here, we will derive the adjoint equation for the mathematical model (28) of the toroidal plasma with axial symmetry. We first derive the adjoint operator for Δ^* defined by (29), then write down the remaining terms, in the axisymmetric toroidal coordinate system, except for the terms associated with the measurement system (the last term in (27)).

In this coordinate system, in carrying out the volume integral, it can be separated into the azimuthal angle ϕ and the other R and Z coordinates, and the azimuthal angle integration from 0 to 2π is simply the multiplication of 2π, and therefore, we will omit this part and write down the integral over the (R, Z) plane. The volume element in Ω_V is denoted by $dV = Rd\phi dRdZ$, and the surface element on $\partial\Omega_V$ is denoted by $d\boldsymbol{S} = dS\boldsymbol{n}$, where $\boldsymbol{n}$ is the surface normal vector on $\partial\Omega_V$. The surface element in the region projected on a poloidal plane, Ω, is denoted by $dA = dRdZ$, and the values of R at the outer and the inner boundary are denoted by $R^+(Z)$ and $R^-(Z)$, respectively.

Specifically, volume integral of an axisymmetric function $f(R,Z)$ over the region Ω_V can be separated into the azimuthal integral over ϕ and the surface integral over the region Ω as follows,

$$\int_{\Omega_V} f(R,Z)dV = \int_0^{2\pi} d\phi \int_\Omega Rf(R,Z)dA \tag{31}$$

From (19) the adjoint operator $\widehat{\Delta}^*$ for the operator Δ^* given by (29) is defined by the following relation

$$\int_{\Omega_V} \chi\,\Delta^*\psi dV = \int_{\Omega_V} \psi\,\widehat{\Delta}^*\chi dV \tag{32}$$

where χ and ψ are functions defined in the region Ω_V and satisfy the boundary condition (30).

In order to derive $\widehat{\Delta}^*$, we start with expressing Δ^* in terms of Laplacian Δ which is a self-adjoint operator. In axisymmetric geometry Δ is defined as

$$\Delta = \frac{\partial^2}{\partial R^2} + \frac{1}{R}\frac{\partial}{\partial R} + \frac{\partial^2}{\partial Z^2} \tag{33}$$

and therefore Δ^* is expressed as follows,

$$\Delta^* = \Delta - \frac{2}{R}\frac{\partial}{\partial R}. \tag{34}$$

Using this expression, the left-hand side of (32) becomes

$$\int_{\Omega_V} \chi \left(\Delta - \frac{2}{R}\frac{\partial}{\partial R}\right)\psi dV = \int_{\Omega_V} \chi \Delta\psi dV - \int_{\Omega_V} \chi \frac{2}{R}\frac{\partial \psi}{\partial R} dV. \tag{35}$$

The second term in the right-hand side of (35) can be transformed as

$$\int_{\Omega_V} \chi \frac{2}{R}\frac{\partial \psi}{\partial R} dV = \int_0^{2\pi} d\phi \int_\Omega 2\chi \frac{\partial \psi}{\partial R} dA = 2\pi \int_\Omega 2[\chi\psi]_{R^-(Z)}^{R^+(Z)} dZ - 2\pi \int_\Omega 2\psi \frac{\partial \chi}{\partial R} dA. \tag{36}$$

Since ψ and χ are zero at the boundary $\partial\Omega_V$, the first term of the right side of (36) vanishes. Using the self-adjoint characteristic of Laplacian Δ, the right-hand side of (35) becomes

$$\begin{aligned}\int_{\Omega_V} \chi \Delta\psi dV - \int_{\Omega_V} \chi \frac{2}{R}\frac{\partial \psi}{\partial R} dV &= \int_{\Omega_V} \psi \Delta\chi dV + \int_{\Omega_V} \psi \frac{2}{R}\frac{\partial}{\partial R}\chi dV \\ &= \int_{\Omega_V} \psi \left(\Delta + \frac{2}{R}\frac{\partial}{\partial R}\right)\chi dV. \end{aligned} \tag{37}$$

Combining (32), (35) and (37), we obtain the following equation

$$\int_{\Omega_V} \chi \Delta^*\psi dV = \int_{\Omega_V} \chi \left(\Delta - \frac{2}{R}\frac{\partial}{\partial R}\right)\psi dV = \int_{\Omega_V} \psi \left(\Delta + \frac{2}{R}\frac{\partial}{\partial R}\right)\chi dV = \int_{\Omega_V} \psi \widehat{\Delta}^*\chi dV \tag{38}$$

from which the expression for the adjoint operator $\widehat{\Delta}^*$ is obtained

$$\widehat{\Delta}^* = \Delta + \frac{2}{R}\frac{\partial}{\partial R} = \Delta^* + \frac{4}{R}\frac{\partial}{\partial R}. \tag{39}$$

Thus, letting $\hat{\psi}(R, Z)$ be the adjoint variable of $\psi(R, Z)$, and using the adjoint operator (39), equation (27) can be written down in axisymmetric cylindrical coordinate system as follows,

$$\begin{aligned}\left(\frac{\partial^2}{\partial R^2} + \frac{3}{R}\frac{\partial}{\partial R} + \frac{\partial^2}{\partial Z^2}\right)\hat{\psi}(R, Z) &= \frac{\partial f}{\partial \psi}\hat{\psi}(R, Z) \\ &+ \frac{\partial f}{\partial \psi(R_{ex}, Z_{ex})}\delta(R - R_{ex}, Z - Z_{ex})\hat{\psi}(R, Z) \\ &+ \Sigma_{i=1}^{N_m} w_i e_i \frac{\partial f_{m_i}}{\partial \psi} \end{aligned} \tag{40}$$

where $\delta(R - R_{ex}, Z - Z_{ex})$ is the two-dimensional delta function in (R, Z) plane, and f is given as follows.

$$f(R, Z) = -\mu_0 R J_\phi(\psi(R, Z), \psi(R_{ex}, Z_{ex}), R, Z) \tag{41}$$

In the last term of the right-hand side in (40), f_{m_i} is an operator associated with the measurement process. Once the expression of this term is obtained in the cylindrical coordinate system, which will be done in the following section V-A, then (40) constitutes the adjoint equation for the target plasma.

C. METHOD for SOLVING the ADJOINT EQUATION

1) BASIC POLICY

In solving the adjoint equation (40) to compute the gradient vector of the cost function, it is desirable to use the same numerical scheme as that used in solving the target GS equation in order to secure the numerical accuracy. There are two major publications about equilibrium reconstruction for RFP plasmas [23] and [24]. In these papers, the GS equation is transformed into an integral equation using the analytic formula of the Green's function of the partial differential operator. Since the GS equation is nonlinear, it is necessary to numerically solve the integral equation by using an iteration scheme.

In this paper, in solving the adjoint equation, we use the method using the Green's function, similar to what is used in [23] and [24] in solving the GS equation. However, it is difficult to derive analytic formula of the Green's function of the derived adjoint operator (39). Therefore, we propose the following method to solve the adjoint equation by using the analytic formula of Green's function of the Laplacian.

2) TRANSFORMATION to INTEGRAL EQUATION WITH GREEN's FUNCTION of LAPLACIAN

The adjoint equation (40) can be transformed into the following partial differential equation (42) with respect to a new variable $\hat{\varphi}$ defined as a product of the adjoint variable $\hat{\psi}$ and radial coordinate R, $\hat{\varphi}(R, Z) = R\hat{\psi}(R, Z)$. After a straightforward calculation, the adjoint equation (40) can be transformed to the following partial differential equation for $\hat{\varphi}(R, Z)$,

$$(\Delta - W(R, Z))\hat{\varphi}(R, Z) = R\rho(R, Z) \tag{42}$$

where $W(R, Z)$ and $\rho(R, Z)$ are defined as

$$W(R, Z) = \frac{1}{R^2} + \frac{\partial f}{\partial \psi(R_{ex}, Z_{ex})}\delta(R - R_{ex}, Z - Z_{ex}) + \frac{\partial f}{\partial \psi} \tag{43}$$

$$\rho(R, Z) = \Sigma_{i=1}^{N_m} w_i e_i \frac{\partial f_{m_i}}{\partial \psi} \tag{44}$$

It should be noted that in (42) the operator acting on $\hat{\varphi}(R, Z)$ does not contain differential operator other than the Laplacian Δ. In such a circumstance, (42) is transformed to the following integral equation for $\hat{\varphi}(R, Z)$ using the Green's function, denoted by G_L, for the Laplacian Δ,

$$\hat{\varphi}(R, Z) = \int_\Omega G_L W(R', Z')\hat{\varphi}(R', Z')R' dA' + \int_\Omega G_L R' \rho(R', Z')R' dA'. \tag{45}$$

G_L corresponds to the electrostatic potential at (R, Z) produced by a unit charge distributed on a toroidal ring located at (R', Z') and is given by the following equation

$$G_L = \frac{1}{2\pi}\sqrt{\frac{R'}{R}} kK(k) \tag{46}$$

where $K(k)$ is the complete elliptic integral of the second kind given as follows

$$K(k) = \int_0^{\frac{\pi}{2}} \frac{d\theta}{[1 - k^2 \sin^2 \theta]^{0.5}} \tag{47}$$

and $k^2 = 4RR'/((R + R')^2 + Z^2)$. Thus we obtain the integral equation (45) which is transformed from the adjoint equation (42).

3) DISCRETIZATION

In order to obtain numerical solution to (45), we discretize it and obtain the matrix expression. Discretize the region Ω into grid points, the number of which is denoted by N and i-th grid point by x_i. Let $\mathbb{G}_L$ be the matrix representation of the Green's function G_L after discretizing the region Ω into grid points. Let $\vec{\rho}$ and $\vec{\hat{\psi}}$ be the vector representation of the function $\rho(R, Z)$ and the adjoint variable $\hat{\psi}$, respectively. The resultant matrix equation for equation (45) becomes

$$\vec{\hat{\psi}} = \mathbb{G}_L \cdot \vec{\rho} + \mathbb{G}_L diag\left(\frac{1}{R(\boldsymbol{x})^2} + \frac{\partial f}{\partial \psi}\right)\vec{\hat{\psi}} + \mathbb{G}_L \mathbb{F}_{ex}\vec{\hat{\psi}} \tag{48}$$

$\mathbb{F}_{ex}$ is the $N \times N$ matrix where the (ex, ex)-th element equals $\partial f(x_{ex})/\partial\psi(x_{ex})$ and all other array elements are equal to 0, where, for simplicity, we assume that the point $\boldsymbol{x}_{ex}$ is equal to one of the grid points, which is denoted by x_{ex} (See equation (30) in reference [23].). The equation (48) can be further modified as follows

$$\vec{\hat{\psi}} - \mathbb{G}_L diag\left(\frac{1}{R(\boldsymbol{x})^2} + \frac{\partial f}{\partial \psi}\right)\vec{\hat{\psi}} - \mathbb{G}_L \mathbb{F}_{ex}\vec{\hat{\psi}} = \mathbb{G}_L \cdot \vec{\rho}. \tag{49}$$

By defining the coefficient matrices as

$$\mathbb{A} = \mathbb{E} - \mathbb{G}_L diag\left(\frac{1}{R(\boldsymbol{x})^2} + \frac{\partial f}{\partial \psi}\right) - \mathbb{G}_L \mathbb{F}_{ex} \tag{50}$$

$$\mathbb{B} = \mathbb{G}_L \cdot \vec{\rho}, \tag{51}$$

we obtain the following matrix equation

$$\mathbb{A}\vec{\hat{\psi}} = \mathbb{B} \tag{52}$$

The adjoint variable $\vec{\hat{\psi}}$ is obtained by solving the matrix equation (52).

V. EXPERIMENTS

It should be noted that the proposed method is applicable to axisymmetric plasmas, including tokamaks and RFPs. Some research programs for the RFP configuration are in progress in the world [25] because of its potential of a compact fusion reactor. In this section, we apply the proposed method of the equilibrium reconstruction to a real RFP plasma in order to evaluate its performance by quantitatively comparing the reconstruction results with those in our previous publication [23]. We conducted the following two experiments. The first one is the numerical experiment in which the proposed algorithm is applied to artificial simulation data, in order to evaluate the accuracy of the proposed method. The second one is the real experiment in which the proposed algorithm is applied to the real experimental data obtained from an RFP experimental device (REversed field Pinch of Low-Aspect-ratio eXperiment (RELAX)) [27] developed at Kyoto Institute of Technology as shown in Fig. 3.

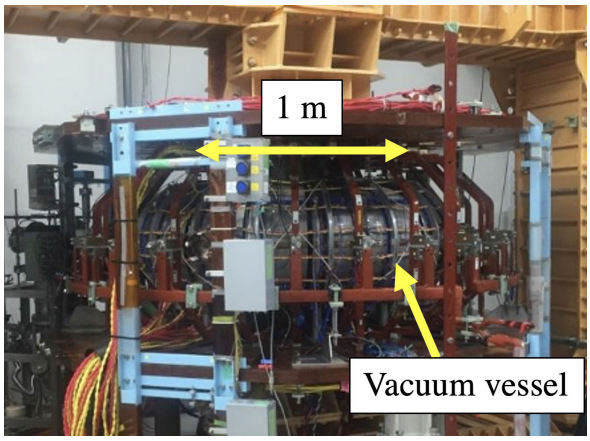

FIGURE 3. A photograph of RELAX device.

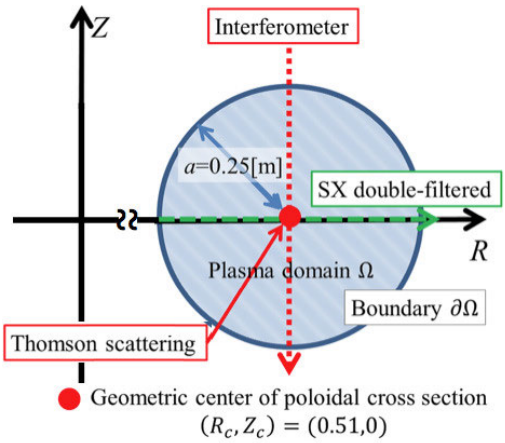

FIGURE 4. Poloidal cross section of the plasma and geometric arrangement of the sensors for plasma data in RELAX.

A. MATHEMATICAL MODEL of RELAX AND ITS SENSING PROCESSES

The mathematical model of the equilibrium of RELAX is described by the partial differential equation (28) and (29), and its boundary condition is described by (30) with $c = 0$. RELAX is equipped with some sensors, and the following six signals are used for equilibrium reconstruction in the experiments. Figure 4 shows a poloidal cross section of the plasma and geometric arrangement of the sensors and sensing processes in RELAX, the major radius R is 0.51 m and minor radius a 0.25m. In the following, we describe the mathematical models (7) for those sensing processes.

Magnetic Sensor 1: The total toroidal plasma current I_ϕ is measured by this sensor. The measurement process is modeled by integration of the toroidal current density J_ϕ over the

poloidal cross section,

$$m_1 = \mathscr{F}_{m_1}(\psi) = \int_\Omega J_\phi(\psi(R,Z),R,Z)dA. \quad (53)$$

Magnetic Sensor 2: The toroidal magnetic flux inside the boundary $\partial\Omega$ is measured by this sensor. The measurement process is modeled as follows,

$$m_2 = \mathscr{F}_{m_2}(\psi) = \frac{1}{\pi a^2}\int_\Omega \frac{F(\psi(R,Z))}{R}dA. \quad (54)$$

Density Sensor 1: The line-averaged electron density is measured by the interferometer [33]. The measurement process is modeled as the line integral of the density in the Z direction at $R = R_c$ divided by the chord length, where (R_c, Z_c) is the geometric center in poloidal cross section of the vacuum vessel as shown in Fig. 4.

$$m_3 = \mathscr{F}_{m_3}(\psi) = (1/2a)\int_{Z_c-a}^{Z_c+a} n(R_c,Z)dZ. \quad (55)$$

Density Sensor 2: The Thomson scattering system measures the electron density at the geometrical center in the poloidal cross section of the vacuum vessel [34]. The measurement process is modeled as follows,

$$m_4 = \mathscr{F}_{m_4}(\psi) = \int_\Omega \delta(R-R_c)\delta(Z-Z_c)n(R,Z)dA. \quad (56)$$

Temperature Sensor 1: The line-of-sight electron temperature is measured by the double-filtered soft-X ray detector [35]. This measurement process is modeled as the line integration of the temperature in the radial (R) direction at $Z = Z_c$ divided by the chord length

$$m_5 = \mathscr{F}_{m_5}(\psi) = (1/2a)\int_{R_c-a}^{R_c+a} T(R,Z_c)dR. \quad (57)$$

Temperature Sensor 2: The Thomson scattering system measures the electron temperature at the geometrical center in the poloidal cross section of the vacuum vessel [34]. It is modeled as follows

$$m_6 = \mathscr{F}_{m_6}(\psi) = \int_\Omega \delta(R-R_c)\delta(Z-Z_c)T(R,Z)dA. \quad (58)$$

B. EXPERIMENTAL RESULTS

In the experiments we adopt the same parametrization method as in our previous paper [23]. In the followings we first explain the parametrization method, and then numerical and experimental results will be shown.

1) PARAMETRIZATION

The unknown parts in the target equation, $F(\psi)$ and $P(\psi)$, should be parametrized by some free parameters. According to the model characterizing the field-aligned current by two parameters, $F' = dF/d\psi$ is expressed as [29]

$$F' = \frac{B_{\phi 0}R_0}{\psi_{max}-\psi_{min}}(1+\frac{1}{\alpha})(1-{\psi_{00}}^{\alpha}) \quad (59)$$

where ψ_{00} are defined as

$$\psi_{00} = \frac{\psi-\psi_{min}}{\psi_{max}-\psi_{min}}.$$

ψ_{min} is the minimum value of ψ, i.e., $\psi_{min} = \min_{\boldsymbol{R,Z}}\psi(R,Z)$ and ψ_{max} is the value of ψ at boundary, i.e., $\psi_{max} = \psi(R,Z)$ at $(R,Z) \in \partial\Omega$. In the target plasma, ψ is generally a monotonic function and becomes maximum at the boundary. $B_{\phi 0}$ is the toroidal magnetic field at the position where ψ takes its minimum value, that is, $B_{\phi 0} = B_\phi(R_{min}, Z_{min})$ where (R_{min}, Z_{min}) is so called the magnetic axis defined by

$$(R_{min}, Z_{min}) = \arg\min_{\boldsymbol{R,Z}} \psi(R,Z). \quad (60)$$

The function F in (28) is determined by integrating F' with value of F at the boundary $F = F(\psi_{max}) = RB_\phi(R,Z)$, $(R,Z) \in \partial\Omega$. Note that $B_\phi(R,Z)$ at $(R,Z) \in \partial\Omega$ is the toroidal magnetic field at the boundary. It is given by a magnetic sensor attached to the plasma boundary in the experiment.

The pressure $P(\psi)$ is expressed by the product of the density $n(\psi(R,Z))$ and the temperature $k_BT(\psi(R,Z))$,

$$P(\psi) = n(\psi)k_BT(\psi) \quad (61)$$

where k_B is the Boltzmann constant. In the above equation, we parameterize the density n and the temperature T as follows

$$n = n_0(1-{\psi_{00}}^{\beta}), \quad (62)$$
$$T = T_0(1-{\psi_{00}}^{\gamma}) \quad (63)$$

where n_0 and T_0 are the density and temperature on the magnetic axis, respectively.

Note that the point $(R,Z) = (R_{min}, Z_{min})$ in (60) satisfies following equations

$$\frac{\partial\psi}{\partial R}(R_{min},Z_{min}) = 0, \quad \frac{\partial\psi}{\partial Z}(R_{min},Z_{min}) = 0. \quad (64)$$

This equation corresponds to the (5) with $c = 0$. In the present work we assume that radial profiles of ion temperature and density are equal to those of electrons. We define

$$\boldsymbol{p} = [B_{\phi 0}, \alpha, n_0, \beta, T_0, \gamma]^t \quad (65)$$

as the free parameters.

2) RESULTS OF NUMERICAL EXPERIMENT

In numerical experiments we generate artificial simulation data $m_1, m_2, \cdots, m_6$ as follows. They are obtained by solving the mathematical model (28), (59), (61), (30) and (64) of the target plasma with the parameters $\boldsymbol{p}$ being given a certain value, denoted by $\boldsymbol{p}_{true}$, and by calculating the sensing processes from (53) to (58) with the solution.

In order to evaluate the proposed method, we conduct numerical experiments with three different methods for searching the minimum value of the cost function (8). One is the proposed method based on the adjoint equation and

TABLE 1. Comparison of p_{true} and obtained values of the free parameter p by the three methods. Initial guess $p = [2, 4.5, 1.3, 5, 3, 5]^t$.

	p_1	p_2	p_3	p_4	p_5	p_6	$E(\boldsymbol{p})$
$\boldsymbol{p}_{true}$	4	3	3	5	4	3	
Proposed Method	4.0005	2.9995	2.9999	5.0002	4.0000	3.0006	7.7081e-09
Method in [23]	4.0002	3.0003	2.9999	4.9998	4.0000	3.0000	9.8945e-09
Amoeba Method	4.0003	2.9991	3.0000	5.0011	3.9998	3.0005	9.6868e-09

TABLE 2. Results of the gradient calculation by the proposed method and the method in [23], and their computational time.

	$\partial E/\partial p_1$	$\partial E/\partial p_2$	$\partial E/\partial p_3$	$\partial E/\partial p_4$	$\partial E/\partial p_5$	$\partial E/\partial p_6$	time for gradient calculation [s]
Proposed Method	-5.119575e-01	-2.008270e-01	-5.493680e-01	-4.666712e-01	-1.034752e-01	-3.572294e-02	0.230
Method in [23]	-5.119311e-01	-2.008303e-01	-5.493634e-01	-4.666600e-01	-1.034732e-01	-3.571167e-02	1.317

second is the method based on the sensitivity equation proposed in [23]; they are gradient-based optimizations. In the experiments, we use the conjugate gradient method (CGM) for these two methods. Third is the Amoeba (downhill simplex) method used in [24], without using the gradients.

We normalize the free parameter $\boldsymbol{p}$ as follows

$$\begin{aligned}\boldsymbol{p} &= [p_1, p_2, p_3, p_4, p_5, p_6]^t \\ &= \left[\frac{B_{\phi 0}}{\widehat{B_{\phi 0}}}, \alpha, \frac{n_0}{\widehat{n_0}}, \beta, \frac{T_0}{\widehat{T_0}}, \gamma\right]^t \end{aligned} \tag{66}$$

where $\widehat{B_{\phi 0}}$, $\widehat{n_0}$, $\widehat{T_0}$ are given as $\widehat{B_{\phi 0}} = 0.1$ T, $\widehat{n_0} = 10^{19}$ m^{-3} and $\widehat{T_0} = 10^6$ K, respectively. In the present numerical experiment, the artificial data $m_1, m_2, \cdots, m_6$ are obtained by giving the value of $\boldsymbol{p}_{true}$ as $[4, 3, 3, 5, 4, 3]^t$. We set the initial guess of $\boldsymbol{p}$ as $[2, 4.5, 1.3, 5, 3, 5]^t$. The weights w_i of the cost function are chosen as $(w_1, w_2, w_3, w_4, w_5, w_6) = (1/d_1^2, 1/d_2^2, 1/d_3^2, 1/d_4^2, 1/d_5^2, 1/d_6^2)$ in order to normalize the contribution from each sensor to the cost function. Table 1 shows $\boldsymbol{p}_{true}$ and the obtained values of the free parameters $\boldsymbol{p}$ by the three methods. Here, we determine that the optimal solution is obtained when the error $E(\boldsymbol{p})$ becomes less than 10^{-8}. It is clearly observed that the parameter $\boldsymbol{p}$ converges to $\boldsymbol{p}_{true}$ with relative errors less than 0.03 % for the three methods. Specifically, the maximum relative error is 0.03 % in p_2 for the Amoeba method, and 0.02 % in p_6 for the proposed method. Moreover, we have also confirmed that the parameter $\boldsymbol{p}$ converges to $\boldsymbol{p}_{true}$ from some other initial guesses.

First we compare the performance of calculating the gradients between the proposed method and the method in our previous paper [23]. Table 2 shows the result of the gradient calculations, in which the values of the gradients obtained at the initial guess are shown together with the computation time for the two methods. The difference in the algorithms for computing gradients between the proposed method and the method in our previous paper [23] is Step 3 and Step 4 in Fig. 1. The time for the gradient calculations in Table 2 means the computational time for performing Step 3 and Step 4 of the proposed method and that for the method in [23] for the corresponding steps. It is observed that the values of the gradient are almost the same between the two methods. The difference appears in the fourth digit of $\partial E/\partial p_6$, the value of which is unity. On the other hand, the computational time of the proposed method is reduced to 0.175 of that of the method in [23]. Note that, in this case the number of the sensitivity equations to be solved in [23] is six and that of the adjoint equation on the proposed method is one.

TABLE 3. Comparison of the number of iterations and the total calculation time, and the avrearged calculation time per unit iteration.

Method	number of iterations	total calculation time	averaged time for gradient calculation
Proposed Method	52	55.777 s	0.138 s
Method in [23]	56	120.15 s	1.223 s
Amoeba Method	446	62.204 s	-

Figure 5 shows an example the convergence behavior of $E(\boldsymbol{p})$ of the proposed method (method based on adjoint method, black line) and the method based on sensitivity equations (magenta line) in our previous paper [23]. For reference, the Amoeba method (cyan line) in [24] is also shown. In the figure, the horizontal axis is the number of iterations and the vertical axis is the value of $E(\boldsymbol{p})$. It is found that in the two gradient-based methods (black and magenta lines) the values of $E(\boldsymbol{p})$ decrease rapidly and the convergence behavior of the two methods is almost the same. On the other hand, in the Amoeba method (cyan line) the convergence is much slower than that of the two gradient-based methods. We compare the iteration numbers and computational time required to reach the optimal solution between those two gradient methods for the result of Fig. 5. Table 3 shows the number of iterations and the total calculation time to obtain the optimal solution, and the avrearged calculation time per one iteration for computing the gradients. For reference, the results obtained by the Amoeba method are also shown. Comparing the two gradient-based methods, the number of iterations to obtain the optimal solution is almost the same: 52 for the proposed method and 56 for the previous method [23]. The total cal-

TABLE 4. Comparison of the real experimental data (Shot No. 20170731007), the outputs of the sensing process obtained from equilibria reconstructed by the proposed and the Amoeba methods.

	measurement data (experimental and reconstructed)						
	plasma current m_1[kA]	average toroidal field m_2[T]	line-averaged electron density $m_3[\mathrm{m}^{-3}]$	central electron density $m_4[\mathrm{m}^{-3}]$	line-of-sight electron temperature m_5[eV]	central electron temperature m_6[eV]	Error
Shot No.20170731007	47.4	1.54×10^{-2}	5.02×10^{18}		37.31	49.64	
Proposed Method	47.4	1.54×10^{-2}	5.02×10^{18}	6.13×10^{18}	37.30	49.64	4.51×10^{-7}
Amoeba Method	47.6	1.53×10^{-2}	5.03×10^{18}	6.64×10^{18}	37.30	49.52	4.27×10^{-5}

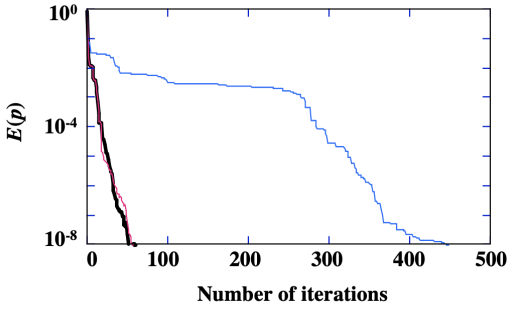

FIGURE 5. Comparison of convergence behavior of the cost function versus the number of iterations among the three methods (Proposed Method: black, Method in [23]: magenta, Amoeba Method: cyan).

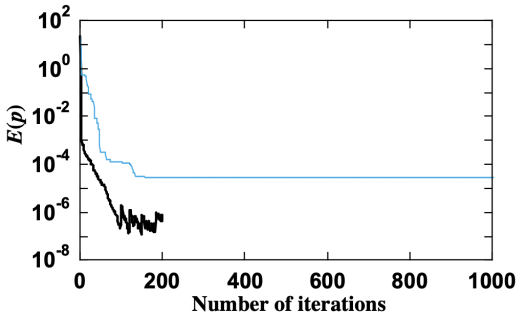

FIGURE 6. Comparison of convergence behavior of the cost function versus the number of iterations between the proposed and the Amoeba methods (Proposed Method: black, Amoeba Method: cyan).

culation time for the proposed method is reduced to less than half of that for the previous method: 55.777 s for the proposed method and 120.15 s for the previous method. In the last column, the average calculation time is shown for the two methods, showing that the reduction in the average gradient computational time from 1.223 s to 0.138 s is the main cause of the reduction in the total calculation time for the proposed method. On the other hand, in the Amoeba method, the number of iterations is 446, much larger than that in the gradient-based methods. However, the total calculation time for the amoeba method is 62.204 s, which is longer than that for the proposed method. From the above comparison, we can conclude that the proposed method based on the adjoint equation is superior to both the previous gradient-based method (based on the sensitivity equation) and the Amoeba method in which gradient calculation is not needed.

3) RESULTS OF REAL EXPERIMENT

We apply the proposed method to the data from the RFP experimental apparatus RELAX developed at Kyoto Institute of Technology. In [23], the reconstruction method based on the sensitivity equation has already been evaluated by applying it to the experimental data for the shot number 20170731007. Here, we apply the proposed method and Amoeba method to the same experimental data and compare the reconstructed results. Table 4 shows the experimental data $(d_1, d_2, \cdots, d_6)$ from RELAX RFP machine, the outputs of the sensing process $(m_1, m_2, \cdots, m_6)$ obtained from reconstructed equilibrium by the proposed method and those by the Amoeba method. In Fig. 6, we compare the convergence behavior of the proposed (black) and Amoeba (cyan) methods. In the reconstruction using the real experimental data, it is found that, with the proposed method, the value of $E(\boldsymbol{p})$ decreases rapidly to 5×10^{-5} after 36 iterations, and further down to 5×10^{-7} after 90 iterations, fluctuating around the minimum value of $E(\boldsymbol{p})$. On the other hand, with the Amoeba method, the value $E(\boldsymbol{p})$ decreases to 5×10^{-5} after 129 iterations, but it never decreases further. That is, the accuracy of the free parameter which provides the optimal equilibrium is much higher for the proposed method than for the Amoeba method. In equilibrium reconstruction using the real experimental data, it is demonstrated that the proposed method based on the adjoint equation has the following great advantage that it brings about much higher accuracy of the reconstructed equilibrium than the conventional Amoeba method.

In order to validate the equilibria reconstructed by the proposed method from perspective of real physical phenomena, we use the same method as in our previous paper [23]. We calculate magnetic fields with reconstructed poloidal magnetic flux ψ. The appropriateness of the reconstructed equilibria is confirmed by comparing the experimental properties of magnetic field fluctuation. We show an example of validation in follows. The profile of the safety factor q is calculated from the reconstructed magnetic field distribution, which is essentially the same as the profile shown with the green line in Fig. 7 of [23]. The calculated value of the on-axis safety factor $q(0)$ is about 0.25 or slightly lower, indicating that the mode rational surface closest to the magnetic axis is $q = 1/5$.

Experimentally, the dominant mode number of fluctuation tends to be $m = 1$, $n = 5$ in the discharge region of the

RELAX plasma. This experimental observation suggests that the innermost mode rational surface is $q = 1/5$, which is consistent with the reconstructed safety factor profile.

VI. CONCLUSION

Equilibrium reconstruction of magnetic fusion plasmas is a fundamental problem for the development of control methods to maintain plasma stability. In this paper we discussed a method for solving the equilibrium reconstruction problem of magnetic fusion plasmas. We developed a method for reconstructing the equilibrium state based on data assimilation which supplements the modeling and analysis with data obtained from equipped devices such as sensors. A reconstruction algorithm based on the adjoint method is proposed in order to significantly reduce the computational time compared to our previous method [23] which is based on the sensitivity equation. The proposed method can be applied to a wide class of axisymmetric magnetic fusion plasmas including the tokamak plasmas, and is expected to play an important role in equilibrium reconstruction of magnetic fusion plasmas. The proposed algorithm is applied to a RELAX RFP machine developed at Kyoto Institute of Technology to evaluate its validity. It is confirmed that the proposed method leads to the results with sufficient accuracy and dramatic reduction of computation time compared with the existing methods.

With advancement of experimental research of fusion plasmas, there may arise new requirements in equilibrium reconstruction methods for both axisymmetric and non-axisymmetric plasmas; in particular, for the development of new methods which have a wider range of applicability in parametrization methods and/or associated numerical algorithms than the existing methods. The method proposed in this paper may have a potential to provide a possible solution to these requirements.

ACKNOWLEDGMENT

The authors would like to thank Dr. R. Paccagnella and Dr. I. Predebon of Consorzio RFX for fruitful discussion, and also would like to thank Prof. H. Himura and T. Okamoto of the Kyoto Institute of Technology for their supports.

REFERENCES

[1] D. J. Ward, N. P. Taylor, and I. Cook, "Economically acceptable fusion power stations with safety and environmental advantages," *Fusion Eng. Design*, vols. 58–59, pp. 1033–1036, Nov. 2001.

[2] W. Manheimer, "Mid century carbon free sustainable energy development based on fusion breeding," *IEEE Access*, vol. 6, pp. 64954–64969, 2018.

[3] B. Bigot, "Preparation for assembly and commissioning of ITER," *Nucl. Fusion*, vol. 62, no. 4, Apr. 2022, Art. no. 042001.

[4] H. Grad and H. Rubin, "Hydromagnetic equilibria and force-free fields," in *Proc. 2nd UN Conf. Peaceful Uses At. Energy*, vol. 31, 1958, pp. 190–197.

[5] V. D. Shafranov, "On magnetohydrodynamical equilibrium configurations," *Sov. Phys. JETP*, vol. 6, no. 3, pp. 545–554, Mar. 1958.

[6] M. Wakatani, *Stellarator and Heliotron Devices*. New York, NY, USA: Oxford Univ. Press, 1988.

[7] L. Bengtsson, *Dynamic Meteorology: Data Assimilation Methods* (Applied Mathematical Sciences), vol. 36. New York, NY, USA: Springer-Verlag, 1981.

[8] M. Sharan, *Data Assimilation and Its Applications*. Basel, Switzerland: Springer, 2012.

[9] M. Asch, *Data Assimilation: Methods, Algorithms, and Applications*. Philadelphia, PA, USA: Society for Industrial and Applied Mathematics, 2016.

[10] Z. H. Ismail and N. A. Jalaludin, "Robust data assimilation in river flow and stage estimation based on multiple imputation particle filter," *IEEE Access*, vol. 7, pp. 159226–159238, 2019.

[11] M. Eltahan and S. Alahmadi, "Numerical dust storm simulation using modified geographical domain and data assimilation: 3DVAR and 4DVAR (WRF-Chem/WRFDA)," *IEEE Access*, vol. 7, pp. 128980–128989, 2019.

[12] L. L. Lao, H. St. John, R. D. Stambaugh, A. G. Kellman, and W. Pfeiffer, "Reconstruction of current profile parameters and plasma shapes in tokamaks," *Nucl. Fusion*, vol. 25, no. 11, pp. 1611–1622, Nov. 1985.

[13] J. R. Ferron, M. L. Walker, L. L. Lao, H. E. S. John, D. A. Humphreys, and J. A. Leuer, "Real time equilibrium reconstruction for tokamak discharge control," *Nucl. Fusion*, vol. 38, no. 7, pp. 1055–1066, Jul. 1998.

[14] J.-M. Moret, B. P. Duval, H. B. Le, S. Coda, F. Felici, and H. Reimerdes, "Tokamak equilibrium reconstruction code LIUQE and its real time implementation," *Fusion Eng. Design*, vol. 91, pp. 1–15, Feb. 2015.

[15] B. S. Yuan, X. Q. Ji, Y. G. Li, Y. Xu, Y. Zhou, L. M. Yu, S. Y. Liang, and T. F. Sun, "Study of plasma equilibrium reconstruction on HL-2A," *Fusion Eng. Design*, vol. 134, pp. 5–10, Sep. 2018.

[16] P. J. McCarthy, P. Martin, and W. Schneider, "The CLISTE interpretive equilibrium code," IPP, Garching, Germany, IPP Rep. 5/85, May 1999.

[17] J. Blum, C. Boulbe, and B. Faugeras, "Reconstruction of the equilibrium of the plasma in a tokamak and identification of the current density profile in real time," *J. Comput. Phys.*, vol. 231, no. 3, pp. 960–980, Feb. 2012.

[18] V. D. Pustovitov, "Magnetic diagnostics: General principles and the problem of reconstruction of plasma current and pressure profiles in toroidal systems," *Nucl. Fusion*, vol. 41, no. 6, pp. 721–730, Jun. 2001.

[19] H. Anand, C. Galperti, S. Coda, B. P. Duval, F. Felici, T. Blanken, E. Maljaars, J.-M. Moret, O. Sauter, T. P. Goodman, and D. Kim, "Distributed digital real-time control system for the TCV tokamak and its applications," *Nucl. Fusion*, vol. 57, no. 5, May 2017, Art. no. 056005.

[20] F. Carpanese, F. Felici, C. Galperti, A. Merle, J. M. Moret, and O. Sauter, "First demonstration of real-time kinetic equilibrium reconstruction on TCV by coupling LIUQE and RAPTOR," *Nucl. Fusion*, vol. 60, no. 6, Jun. 2020, Art. no. 066020.

[21] J. W. Berkery, S. A. Sabbagh, L. Kogan, D. Ryan, J. M. Bialek, Y. Jiang, D. J. Battaglia, S. Gibson, and C. Ham, "Kinetic equilibrium reconstructions of plasmas in the MAST database and preparation for reconstruction of the first plasmas in MAST upgrade," *Plasma Phys. Controlled Fusion*, vol. 63, no. 5, May 2021, Art. no. 055014.

[22] Y. Jiang, S. A. Sabbagh, Y. S. Park, J. W. Berkery, J. H. Ahn, J. D. Riquezes, J. G. Bak, W. H. Ko, J. Ko, J. H. Lee, S. W. Yoon, A. H. Glasser, and Z. R. Wang, "Kinetic equilibrium reconstruction and the impact on stability analysis of KSTAR plasmas," *Nucl. Fusion*, vol. 61, no. 11, Nov. 2021, Art. no. 116033.

[23] A. Sanpei, T. Okamoto, S. Masamune, and Y. Kuroe, "A data-assimilation based method for equilibrium reconstruction of magnetic fusion plasma and its application to reversed field pinch," *IEEE Access*, vol. 9, pp. 74739–74751, 2021.

[24] J. K. Anderson, C. B. Forest, T. M. Biewer, J. S. Sarff, and J. C. Wright, "Equilibrium reconstruction in the Madison symmetric torus reversed field pinch," *Nucl. Fusion*, vol. 44, no. 1, pp. 162–171, Jan. 2004.

[25] L. Marrelli, P. Martin, M. E. Puiatti, J. S. Sarff, B. E. Chapman, J. R. Drake, D. F. Escande, and S. Masamune, "The reversed field pinch," *Nucl. Fusion*, vol. 61, no. 2, Feb. 2021, Art. no. 023001.

[26] S. Ortolani and D. D. Schnack, *Magnetohydrodynamics of Plasma Relaxation*. Singapore: World Scientic, 1993.

[27] S. Masamune, A. Sanpei, R. Ikezoe, T. Onchi, K.-I. Murata, K. Oki, H. Shimazu, T. Yamashita, and H. Himura, "Characterization of initial low-aspect ratio RFP plasmas in 'RELAX,'" *J. Phys. Soc. Jpn.*, vol. 76, no. 12, Dec. 2007, Art. no. 123501.

[28] V. Antoni, D. Merlin, S. Ortolani, and R. Paccagnella, "MHD stability analysis of force-free reversed field pinch configurations," *Nucl. Fusion*, vol. 26, no. 12, pp. 1711–1788, Dec. 1986.

[29] R. Paccagnella, A. Bondeson, and H. Lütjens, "Ideal toroidal stability beta limits and shaping effects for reversed field pinch configurations," *Nucl. Fusion*, vol. 31, no. 10, pp. 1899–1908, Oct. 1991.

[30] M. Zuin, "Ion temperature measurements by means of a neutral particle analyzer in RFX-mod plasmas," in *Proc. 38th EPS Conf. Plasma Phys.*, Strasbourg, France, Jun./Jul. 2011 pp. 1–4.
[31] E. Scime, M. Cekic, D. J. Den Hartog, and S. Hokin, "Ion heating and magnetohydrodynamic dynamo fluctuations in the reversed-field pinch," *Phys. Plasmas*, vol. 4, p. 4062, Aug. 1992.
[32] R. Gatto and P. W. Terry, "Anomalous ion heating from ambipolar-constrained magnetic fluctuation-induced transport," *Phys. Plasmas*, vol. 8, no. 3, pp. 825–835, Mar. 2001.
[33] M. Sugihara, K. Oki, R. Ikezoe, T. Onchi, A. Sanpei, H. Himura, S. Masamune, T. Akiyama, A. Ejiri, K. Sakamoto, K. Nagasaki, and V. Zhuravlev, "Density regimes of low-aspect-ratio RFP plasmas in RELAX," *Plasma Fusion Res.*, vol. 5, pp. S2061–S2061, 2010.
[34] R. Ueba, S. Masamune, A. Sanpei, K. Uchiyama, H. Tanaka, K. Nishimura, G. Ishii, R. Kodera, H. Himura, D. J. D. Hartog, and H. Koguchi, "Electron temperature measurement by Thomson scattering in a low-aspect-ratio RFP RELAX," *Plasma Fusion Res.*, vol. 9, 2014, Art. no. 1302009.
[35] K. Nishimura, A. Sanpei, H. Tanaka, G. Ishii, R. Kodera, R. Ueba, H. Himura, S. Masamune, S. Ohdachi, and N. Mizuguchi, "2D electron temperature diagnostic using soft X-ray imaging technique," *Rev. Sci. Instrum.*, vol. 85, no. 3, Mar. 2014, Art. no. 033502.

AKIO SANPEI (Member, IEEE) received the B.Sc., master's, and Ph.D. degrees from Kyoto University, Kyoto, Japan, in 1999, 2001, and 2004, respectively.

In 2004, he joined the Department of Electronics, Kyoto Institute of Technology, Kyoto, as an Assistant Professor, where he became a Lecturer, in 2014, and he has been an Associate Professor, since 2019. His current research interests include plasma science, dusty plasmas, fusion plasma, and nonneutral plasma.

SADAO MASAMUNE received the B.Eng., M.Eng., and Ph.D. degrees in nuclear engineering from Kyoto University, Kyoto, Japan, in 1976, 1978, and 1984, respectively.

In 1982, he joined the Kyoto Institute of Technology (KIT), Kyoto, as an Assistant Professor, and was promoted to an Associate Professor, in 1988. He was a Visiting Scientist with the Los Alamos National Laboratory, from 1985 to 1986, and in 1989. He was a Visiting Scientist with Kernfroshungsanlage Jülich, in 1987. He was a Visiting Faculty Member of the University of Wisconsin-Madison, in 1996. From 2000 to 2019, he was a Full Professor with KIT. He was a Visiting Professor with the National Institute for Fusion Science (NIFS), from 2010 to 2011. He was a Visiting Professor with the Institute of Advanced Energy, Kyoto University, in 2012. In 2019, he joined the College of Engineering, Chubu University, Kasugai, Japan, as a Full Professor. His research interests include fusion plasma science, with emphasis on MHD phenomena associated with relaxation or self- organization in fusion plasmas.

YASUAKI KUROE (Life Member, IEEE) received the B.S. and M.S. degrees in instrumentation engineering and the Ph.D. degree in industrial science from Kobe University, Kobe, Japan, in 1974, 1977, and 1982, respectively. In 1982, he joined the Department of Electrical Engineering, Kobe University, as an Assistant Professor. In 1991, he moved to the Department of Electronics and Information Science, Kyoto Institute of Technology, Kyoto, Japan, as an Associate Professor, and became a Professor. Since 2016, he has been a Professor Emeritus with the Kyoto Institute of Technology. He is currently a Visiting Professor with the Faculty of Engineering Science, Kansai University, Osaka, Japan, and a Research Fellow with Doshisha University, Kyoto. His current research interests include computational intelligence, control and system theory and its applications, and computer-aided analysis and design.